An Inverter-Based Flexible Microgrid Grounding Scheme

Dingrui Li, *Member, IEEE*, Yiwei Ma, *Member, IEEE*, Yu Su, *Student Member, IEEE*, Chengwen Zhang, *Member, IEEE*, Lin Zhu, *Senior Member, IEEE*, He Yin, *Senior Member, IEEE*, Fred Wang, *Fellow, IEEE*, and Leon M. Tolbert, *Fellow, IEEE*

***Abstract*—Due to multiple operation modes and corresponding mode transitions of microgrids (MGs), the MG grounding design is challenging. An MG may lose its grounding provided by the main distribution grid when it transitions to the islanded operation, resulting in potential hazards to both equipment and personnel. Existing transformer-based grounding schemes are bulky and have low control capability, which leads to poor transition performances and may affect the operation and protection of the whole distribution grid in the grid-connected mode. Power inverters have been applied as interfaces of distributed energy resources (DERs), which can potentially serve as groundings for future MGs. In this article, a novel DER inverter-based MG grounding scheme is proposed to realize flexible grounding in MGs. The detailed grounding structure and control methods are discussed. The proposed grounding scheme is verified on a realistic MG model through simulation. The proposed control strategies are demonstrated on a converter-based hardware testbed.**

***Index Terms*—Distributed energy resources, inverter, microgrid grounding, mode transition.**

Nomenclature

PS, NS, ZS	Positive, negative, and zero sequences.
$\vec{V}_p$, $\vec{V}_{\text{pn}}$, $\vec{V}_{\text{ng}}$	Normalized phasor representations of phase voltage, phase-to-neutral voltage, and neutral-to-ground voltage.
$\vec{I}_{0\text{tot}}$, $\vec{I}_{0\text{max}}$, $\vec{I}^{f}_{0\text{max}}$	Normalized phasor representations of total load ZS current, maximum load ZS current, and maximum fault ZS current.
$\vec{I}_{\text{DT}}$, $\vec{I}_{\text{DER}}$	Normalized phasor representations of total DER transformer current and rated DER current.
Z_{NFE}, Z_G, Z_{line}, Z_T	Normalized NFE impedance, grounding impedance between neutral and earth, line impedance, and DER transformer impedance.
$T^{\text{max}}_{\text{TOV}}$	Maximum allowed TOV duration.
ω_{cut}, ω	Cut-off and resonant frequencies in PR controller.
MG, DER	Microgrid and distributed energy resources.
TOV	Temporary over-voltage.
LV, MV	Low-voltage and medium-voltage.
GFM, GFL	Grid-forming and grid-following.
NFE	Neutral forming equipment.

Manuscript received 12 September 2023; revised 14 December 2023 and 22 February 2024; accepted 24 April 2024. Date of publication 1 May 2024; date of current version 20 June 2024. This work was supported in part by the Advanced Research Projects AgencyEnergy (ARPA-E) under Grant DE-AR0000665, in part by the Engineering Research Center Program of the National Science Foundation and DOE for the use of Engineering Research Center Shared Facilities under NSF Award EEC1041877, and in part by the CURENT Industry Partnership Program. Recommended for publication by Associate Editor C. Fernandez. *(Corresponding author: Dingrui Li.)*

Dingrui Li, Yiwei Ma, Yu Su, Chengwen Zhang, Lin Zhu, He Yin, and Leon M. Tolbert are with the Department of Electrical Engineering and Computer Science, University of Tennessee, Knoxville, TN 37996 USA (e-mail: dli35@vols.utk.edu; myiwei@gmail.com; ysu10@utk.edu; zcwham@gmail.com; lzhu12@utk.edu; hyin8@utk.edu; tolbert@utk.edu).

Fred Wang is with the Department of Electrical Engineering and Computer Science, University of Tennessee, Knoxville, TN 37996 USA, and also with Oak Ridge National Laboratory, Oak Ridge, TN 37830 USA (e-mail: f.wang@ieee.org).

Color versions of one or more figures in this article are available at https://doi.org/10.1109/TPEL.2024.3395614.

Digital Object Identifier 10.1109/TPEL.2024.3395614

I. Introduction

In A distribution electric grid, system grounding plays an important role. According to IEEE Std. 142-2007 [1], grounding is applied to limit system voltage with respect to the earth and provide a path for ground fault current, which will impact the system operation under both normal and fault conditions. During normal conditions, no grounding means no zero-sequence (ZS) current path, which may affect the operation of single-phase loads. During unbalanced ground fault conditions, no grounding indicates no path for ZS ground fault current, which will increase the complexity of ground fault detection and result in high temporary overvoltage (TOV) that may damage the insulation of equipment and increase the risk of electric shock to personnel.

A grounding scheme of a three-phase grid contains neutral-forming equipment (NFE) and a grounding connection from neutral to ground. The NFE forms a valid neutral that can be used to provide a ZS current path for the unbalanced load and unbalanced ground fault currents [2]. The grounding connection determines how the neutral is connected to the earth, including solid connection, resistance connection, etc. The grounding connection will impact the magnitude of the ground fault current and TOV [3]. One widely applied system grounding scheme is shown in Fig. 1, where the distribution feeder is grounded through a delta-wye (Δ-Yg) connected transformer with a low-resistance grounding connection [1]. The Δ-Yg transformer is NFE, and the low-impedance connection limits the TOV during ground fault conditions.

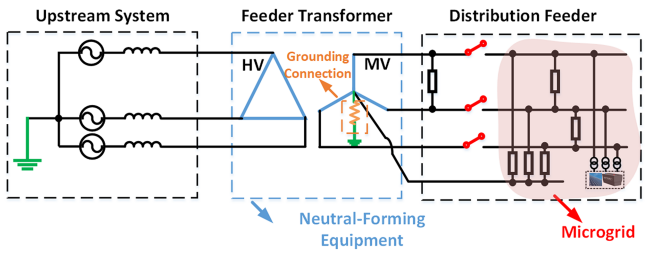

Fig. 1. System grounding illustration.

A microgrid (MG) is a group of localized loads and distributed energy resources (DERs) that have two operation modes: grid-connected mode and islanded mode [4], [5], [6]. In the grid-connected mode, the grounding of an MG is usually provided by the feeder transformer as shown in Fig. 1. However, when the MG is islanded, the MG will very often lose the grounding and face the risk of abnormal operation. Moreover, with the increased integration of DERs, future MGs will have multiple DERs at different locations, leading to multiple sub-MGs [7]. In this condition, each sub-MG is also required to be grounded when it operates independently.

To solve this practical issue, two approaches have been reported in the existing literature. The first one is the DER transformer-based grounding scheme [8], which can be viewed as a multineutral solution. DERs are usually connected to the MG through step-up transformers. By changing the transformer connection to Δ (LV)-Yg (MV), the DER transformer can provide an extra neutral and ZS current path to serve as a grounding of the MG. However, when the MG is in the grid-connected mode, this approach will result in extra paths for ZS currents, which changes the ZS current distribution of the whole grid and desensitizes the protection of the main distribution grid, especially existing ZS current-based protection. An MG is usually developed based on an existing feeder where system settings such as protection parameters are determined through numerous field tests or simulations. Therefore, redesigning the protection solely for the purpose of grounding coordination will require excessive engineering effort and cost that can be hardly justified economically.

The second approach is a single neutral solution that adds a dedicated grounding transformer for use only in the islanded mode, which is disconnected through a mechanical switch in grid-connected mode. This approach is adopted in the Duke Energy MG in North Carolina [9] and EPB MG in Chattanooga, Tennessee [10], which provides a grounding in islanded mode and avoids impacts on the whole distribution grid in the grid-connected mode. However, grounding transformers are bulky and lossy, and the switching speed of the mechanical switch is slow, which impacts the smoothness of MG mode transitions (from grid-connected to islanded and vice versa). Furthermore, for the MG with multiple sub-MGs, this approach greatly increases the cost, loss, and transition complexity.

Existing MG grounding schemes in [8], [9], and [10] are based on transformers that are bulky and have low control flexibility. In this article, an inverter-based scheme is considered as a candidate for future MG grounding. In the existing literature, power inverters, especially four-wire ones, have been applied for unbalanced load support [11], [12], [13]. Voltage and current control strategies for a four-wire grid-forming (GFM) inverter with split capacitor topology to support unbalanced loads in urban rail trains are proposed in [11]. An optimal design of the filter and neutral inductors for four-wire GFM inverters for unbalanced load support is proposed in [12]. The neutral current compensation capability is enhanced in [13] by fully utilizing the capacity of a four-wire grid-following (GFL) compensator. However, existing research either assumes that the grounding and neutral are provided by the system or focuses on unbalance support for a single load section. There is no literature that uses the inverter to serve as the grounding for a system, especially an MG, where system-level requirements from different MG operation conditions as well as mode transitions need to be considered for grounding implementation.

Therefore, in this article, an inverter-based grounding scheme is proposed to flexibly form the neutral and ground an islanded MG. By realizing the MG grounding with DER inverters, the following benefits can be achieved.

1) No need for additional bulky grounding transformers.
2) A flexible grounding scheme can be realized through inverter control to avoid grounding impacts on the main distribution grid in the grid-connected mode.
3) Grounding availability can be determined by the inverter control so that fast grounding transitions can be realized to smooth the MG mode transition.

The rest of this article is organized as follows: In Section II, the MG concept and grounding requirements are introduced. Existing MG grounding schemes are covered in Section III. The proposed grounding scheme is detailed in Section IV. Section V provides the simulation verification, and experimental demonstration is provided in Section VI. Finally, conclusions are drawn in Section VII.

II. MG Concept and Grounding Requirements

A. MG With Multiple Source Locations

In recent years, due to increased integration of DERs and smart switches, the MG with multiple source locations has been developed, which can either serve as a merged MG or separate into multiple sub-MGs. This type of MG further increases the flexibility and resiliency of the grid. As shown in Fig. 2, when all the smart switches are opened, there will be n separated sub-MGs, meaning that each sub-MG will need its own grounding. Furthermore, this MG contains more transitions, including sub-MG separation (from a merged MG to separated sub-MGs) and sub-MG merging (inverse transition from multiple sub-MGs to fewer sub-MGs), which leads to more impacts on the grounding implementation.

B. MG Grounding Requirements

1) Steady-State Requirements: In a three-phase system, the unbalanced voltage or current can be decomposed into PS, NS, and ZS components. The unbalanced load will result in PS, NS,

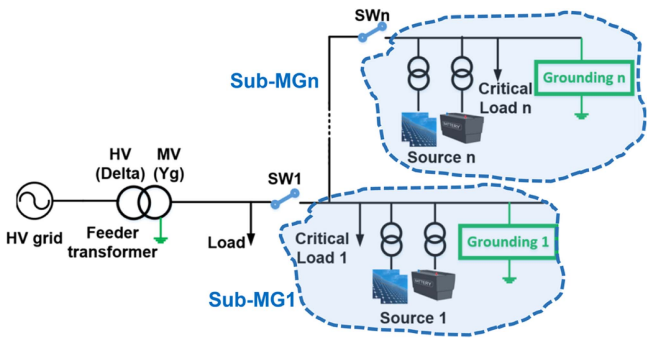

Fig. 2. MG with multiple source locations.

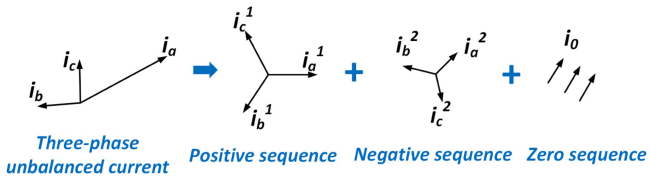

Fig. 3. Symmetrical decomposition of three-phase unbalanced current.

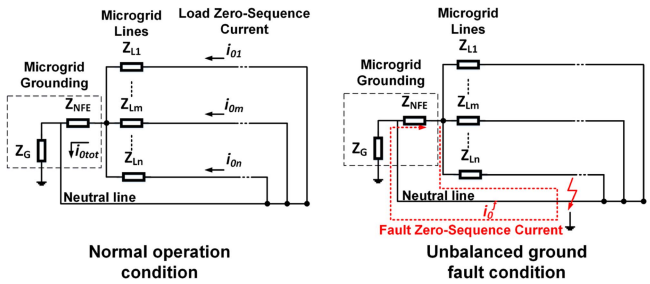

Fig. 4. ZS circuit of an MG in normal and fault conditions.

and ZS currents as shown in Fig. 3. Compared with PS and NS components, the ZS components will not be canceled among three phases, which require a neutral point and a fourth wire to flow through. The neutral point and the fourth wire are provided by the system grounding.

Due to the line and NFE impedances, the flow of ZS current will cause ZS voltage, which will cause voltage unbalance in the MG. From the existing literature, the voltage unbalance can be defined by the ratio of NS voltage and PS voltage [14] or the maximum voltage amplitude deviation to the average voltage amplitude [15]. However, neither of these definitions clearly describes the impacts of ZS voltage. The voltage unbalance caused by the ZS voltage affects the equipment insulation design and personnel safety. In this article, the ZS voltage requirement is defined by the single phase-to-ground voltage range [14], meaning that the phase-to-ground voltage should not exceed the normal operation range defined in (1) when ZS voltage deviation is considered

$$0.95\ p.u. \leq \left|\vec{V}_p\right| \leq 1.05\ p.u. \tag{1}$$

The ZS equivalent circuit of an MG is described in Fig. 4, where Z_G is the grounding impedance between neutral and earth, and Z_{NFE} is the ZS impedance of NFE. All the ZS currents will flow into the neutral and back to the load. The voltage drop on Z_{NFE} will result in a voltage shift of the neutral point, causing phase-to-ground voltage unbalance. The neutral voltage shift is

$$\vec{V}_{\mathrm{ng}} = \vec{I}_{0\mathrm{tot}}\ \vec{Z}_{\mathrm{NFE}}. \tag{2}$$

The phase-to-ground voltage is described as

$$\vec{V}_p = \vec{V}_{\mathrm{pn}} + \vec{V}_{\mathrm{ng}}. \tag{3}$$

According to (1)–(3), the NFE impedance design requirement is

$$0.95 \leq \left|\vec{V}_{\mathrm{pn}} + \vec{I}_{0\mathrm{max}}\vec{Z}_{\mathrm{NFE}}\right| \leq 1.05. \tag{4}$$

2) Fault Requirements: During unbalanced ground fault conditions, as shown in Fig. 4, the ZS current will flow through the neutral and grounding impedance (Z_G), then back to the fault location. Before the MG protection responds, the high fault ZS current will lead to a high neutral voltage shift, resulting in the TOV in the healthy phases. An effective grounding is needed to limit the TOV during unbalanced ground faults to protect equipment and personnel; according to [16], for a system with effective grounding, the fault TOV requirement is

$$\mathrm{TOV} \leq 1.38\ p.u. \tag{5}$$

The NFE impedance requirement is described as

$$\left|\vec{V}_{\mathrm{pn}} + \vec{I}^{f}_{0\mathrm{max}}\left(\vec{Z}_{\mathrm{NFE}} + \vec{Z}_G + \vec{Z}_{\mathrm{line}}\right)\right| \leq 1.38. \tag{6}$$

If there is no grounding in the MG, during the single phase-to-ground fault condition, the phase-to-ground voltage of healthy phases can be up to the line voltage.

3) Transition Requirements: Due to multiple operation modes, an MG has different types of transitions, including black start, planned/unplanned islanding, reconnection, planned/unplanned sub-MG separation, and sub-MG merging. During mode transitions, if the MG grounding transition needs to be implemented, the MG may temporarily lose the grounding during transitions like islanding and separation, which may also result in TOV. Both the amplitude and duration of the TOV should be considered. For example, the duration of TOV in (5) is the fault clearing time, of which the typical value is 0.2 s [17]. Therefore, to limit the transition TOV impacts, the duration of transitions needs to be limited as

$$T_{\mathrm{trans}} \leq T^{\mathrm{max}}_{\mathrm{TOV}}. \tag{7}$$

The TOV caused by transitions is determined by the load and source conditions in the MG, which may be as severe as the ground fault condition. Therefore, the maximum allowed TOV duration should be no greater than 0.2 s. Combining with the MG features, the overall requirements of mode transitions on MG grounding can be summarized as follows.

1) Providing all the MG/sub-MG with grounding before and after transitions.
2) Minimizing the added MG grounding impacts on the main distribution grid.
3) Limiting the transition duration to less than the maximum allowed TOV duration.

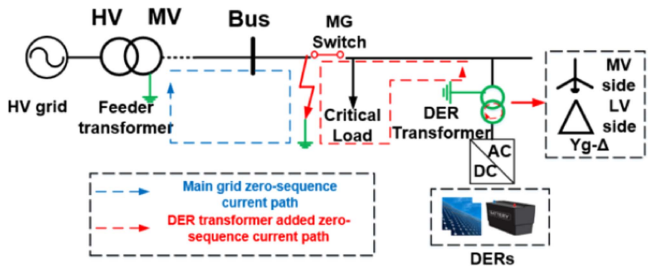

Fig. 5. DER transformer-based MG grounding scheme.

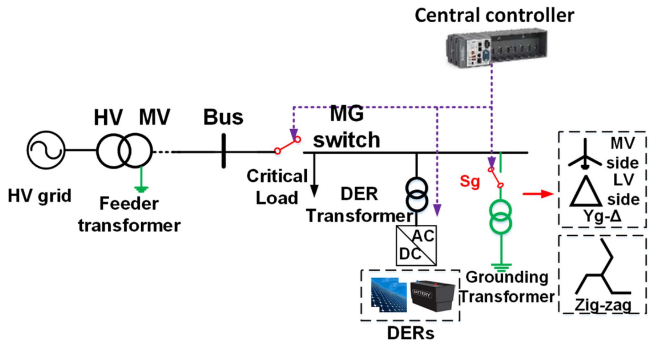

Fig. 6. Grounding transformer-based MG grounding scheme.

III. Existing MG Grounding Schemes

A. Multineutral Solution

For the multineutral solution, one example is to ground the MG through the Δ-Yg connected DER transformer. As shown in Fig. 5, at the DER side, the ZS current circulates within the delta connection and no ZS current will flow into the DER.

The DER transformer-based grounding scheme does not require extra equipment for MG grounding. Also, it is connected to the MG during different operation modes so that there is no TOV caused by no grounding during transitions. However, the DER transformer-based grounding is connected in the grid-connected mode, resulting in multiple neutrals in the whole distribution grid and providing extra ZS current paths, which will affect the operation of the main distribution grid, especially during ground fault conditions.

During the unbalanced ground fault condition, the ZS current paths for an MG with a single source are summarized in Fig. 5. The neutral from the DER transformer adds one more path for the ZS current. The fault ZS current at the grid side will be changed to desensitize the ZS current-based protection of the main grid and increase the risk of overvoltage to equipment and personnel. This issue will be more severe in an MG with multiple source locations because multiple added groundings will cause multiple additional ZS current paths to further desensitize the protection of the main grid.

B. Single Neutral With Transitions Solution

To provide a grounding in the islanded mode and minimize the impacts on the main grid, the single neutral with transition solution is applied. One representative example is the grounding transformer with an isolation switch [9], [10]. As shown in Fig. 6, an isolation switch S_g is added to disconnect the grounding transformer in grid-connected mode [9], which can circumvent the grounding transformer's impacts on the grid-connected operation. However, challenges exist during mode transitions. Once grounding transformers are required to be connected or disconnected during mode transitions, switch S_g needs to coordinate with the MG controller and protection through communication, requiring high-speed communication. Meanwhile, switch S_g is normally a mechanical switch. The switching actions of mechanical switches slow down the grounding transitions. The transition performances will be discussed based on the timelines in Fig. 7.

For the transitions of black start, reconnection, and planned islanding, the transition schedule is known, meaning that the MG controller is able to connect or disconnect the grounding transformer before or after the transition happens to avoid ungrounded conditions as shown in Fig. 7. However, the grounding switching will slow the transition process. During planned islanding and reconnections, there will be a temporary multineutral condition. If a ground fault happens simultaneously, the grid-side protection will also be impacted.

During the unplanned islanding transition (usually triggered by faults), since the islanding schedule is unknown, the grounding switching will cause more severe impacts. As shown in Fig. 7, islanding occurred at t_1 and was detected at t_2. The central controller issued grounding transition commands to connect the grounding transformer, which arrived at t_3 due to the communication delay, and S_g started to close. After the switching action finished, the islanding transition finished at t_4. During t_1–t_4, the MG is ungrounded because the main grid is disconnected and the grounding transformer has not been connected, which may cause TOV if a ground fault occurs. Δt_{12} is the islanding detection time, which is determined by the islanding detection method. Δt_{23} is the communication delay, and Δt_{34} is the switching action delay. According to the transition requirement, the transition duration requirement is

$$\Delta t_{12} + \Delta t_{23} + \Delta t_{34} \leq T_{\text{TOV}}^{\max}. \tag{8}$$

In the actual MG, the central controller can be located far from the grounding transformer and the communication delay will be long (up to several seconds). In addition, the switching actions of mechanical switches will at least take several line cycles [18]. Therefore, the grounding transformer-based single neutral solution is not likely to meet the short TOV duration requirement during transitions, meaning that the MG may need to shut down and black start to reach islanded operation.

For an MG with multiple sub-MGs, each separate sub-MG needs its own grounding transformer and isolation switch, which increases the total cost. During the island separation and merging transitions, grounding transitions may also need to be considered. The timeline of the merging transition is similar to reconnection and the timeline of the separation transition is similar to the islanding. Thus, during the unplanned separation

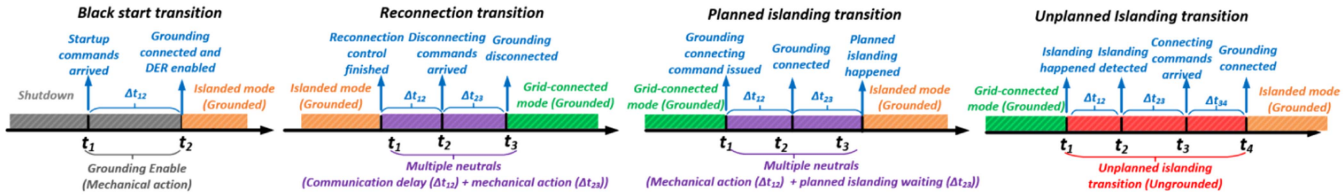

Fig. 7. Grounding transitions' timeline for the existing single neutral scheme.

transition, the grounding transformer-based approach may not meet the TOV duration requirement, either.

Therefore, for the single neutral solution, the grounding transitions will result in TOV during unplanned islanding and unplanned separation transitions, and the transition TOV duration requirement cannot be met.

IV. Proposed Inverter-Based Grounding Scheme

To solve the issues of existing grounding schemes in MG operation and mode transitions, an inverter-based grounding scheme is proposed, which is a single neutral solution with better transition performances. In this section, the overall structure of the proposed grounding scheme is introduced first. Then the implementation methodology is described. Finally, the control algorithms for the proposed grounding are stated.

A. Proposed Grounding Scheme

The proposed grounding structure is shown in Fig. 8. DER inverters work as sources of MGs and sub-MGs, meaning that no additional equipment is needed for grounding purposes. In the proposed grounding scheme, the connection of the DER transformer is selected to be a Yg-Yg connection. The ZS equivalent circuit of the Yg-Yg connected DER transformer can be modeled as an impedance, which will neither provide a closed loop for ZS current nor block the ZS current. Therefore, the ZS current path is determined by the DER inverter.

Compared with the grounding transformer approach, the proposed approach does not need extra equipment but requires four-wire DER inverters to provide ZS current paths. Four-wire DER inverters can potentially provide ZS current path to work as the NFE and offer the grounding to the MG [19]. There are multiple inverter topologies that can realize the fourth wire of the inverter. Taking two-level voltage source inverters as an example, in the existing literature, four-leg topology and split dc-link capacitor topology are two common use cases for the fourth wire implementation [20], [21].

The overall ZS equivalent circuit of the proposed grounding scheme is shown in Fig. 8. The DER transformer is modeled by its equivalent ZS impedance. The DER inverter is represented by its ZS Thevenin equivalent circuit. The ZS performance of the inverter is determined by the inverter control, which brings high flexibility to the grounding purpose. Inverters can regulate the equivalent output ZS impedance to enable or disable the grounding. When the grounding is disabled such as in the grid-connected mode, the DER inverters can regulate the ZS current to be zero so that the inverter

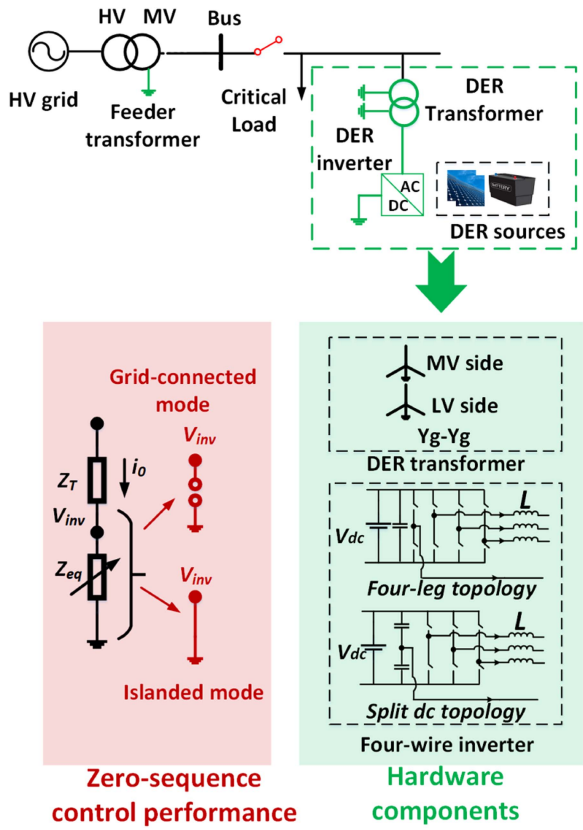

Fig. 8. Proposed DER inverter-based MG grounding scheme.

ZS impedance is infinite and no ZS current path will be provided. When the grounding is enabled, the inverter can regulate its ZS impedance to zero to serve as the grounding of the MG.

B. Implementation of the Proposed Grounding Scheme

The implementation flow chart is shown in Fig. 9, which includes the DER transformer selection and DER inverter selection. MG information is gathered first, including the system load conditions, maximum ZS currents, and the system configuration information. The DER transformer selection includes the continuous rating selection, thermal rating selection, and impedance selection. The continuous rating selection is determined by the steady-state DER current rating, which can be written as

$$\left|\vec{I}_{\mathrm{DT}}\right| \geq \left|\vec{I}_{\mathrm{DER}}\right| + \left|\vec{I}_{0\max}\right|. \tag{9}$$

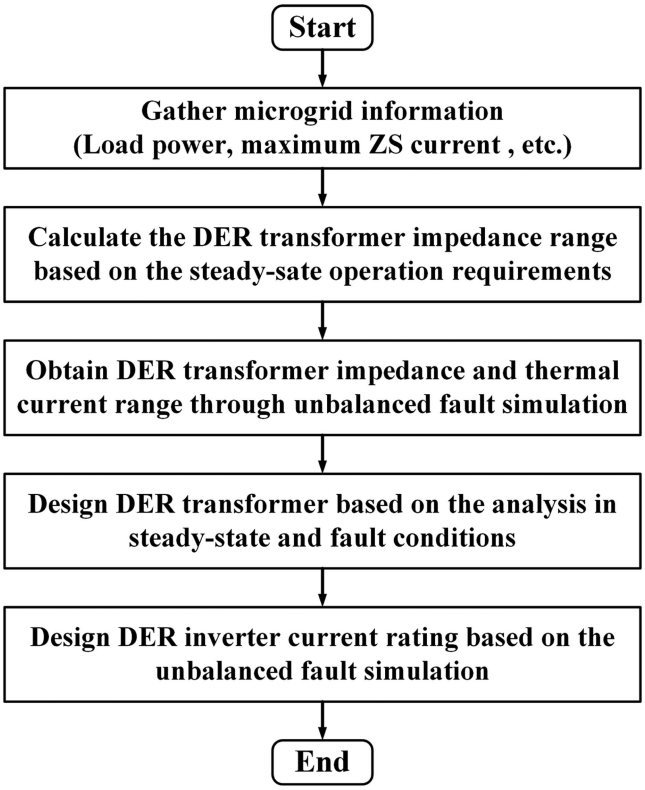

Fig. 9. Implementation methodology of the proposed grounding scheme.

As for the DER transformer impedance selection, it is necessary to take into consideration the steady-state MG voltage requirements and the TOV requirement during fault conditions. The steady-state requirements include the voltage unbalance requirement in (4) and the voltage drop requirement. The voltage drop requirement indicates that the voltage drop on the DER transformer needs to be limited. It can be described as

$$0.95 \leq \left| \vec{V}_p + \vec{I}_{\mathrm{DER}} Z_T \right| \leq 1.05. \tag{10}$$

Note that this requirement is different from (4). The requirement for ZS voltage is in (4) while (10) is the requirement for overall voltage. During fault conditions, the DER transformer impedance is part of the ZS circuit and will affect the TOV. Meanwhile, the DER transformer impedance will also impact the fault current. The DER transformer requirement in the ground-fault condition is obtained through design simulations. By sweeping the DER transformer impedance, the DER transformer impedance can be obtained considering the TOV requirement. Together with the impedance requirement from (4) and (10), the DER transformer impedance can be selected. After the DER transformer impedance is selected, the thermal rating of the DER transformer can also be selected.

After the DER transformer is selected, the DER inverter rating can also be selected. The inverter current rating is determined by the fault current rating, and the inverter voltage requirement should be greater than the TOV. Moreover, the maximum fault ZS current can be used for the design of split dc-link capacitor or the fourth leg. Moreover, the four-wire inverters and DER transformers in the proposed grounding scheme can be different commercial products as long as the inverters and transformers meet the grounding requirements. Therefore, the loss and efficiency of the scheme are determined by the commercial product selection.

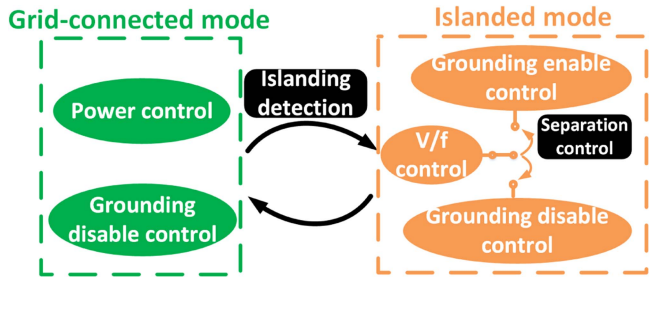

Fig. 10. Control logic for the DER inverter.

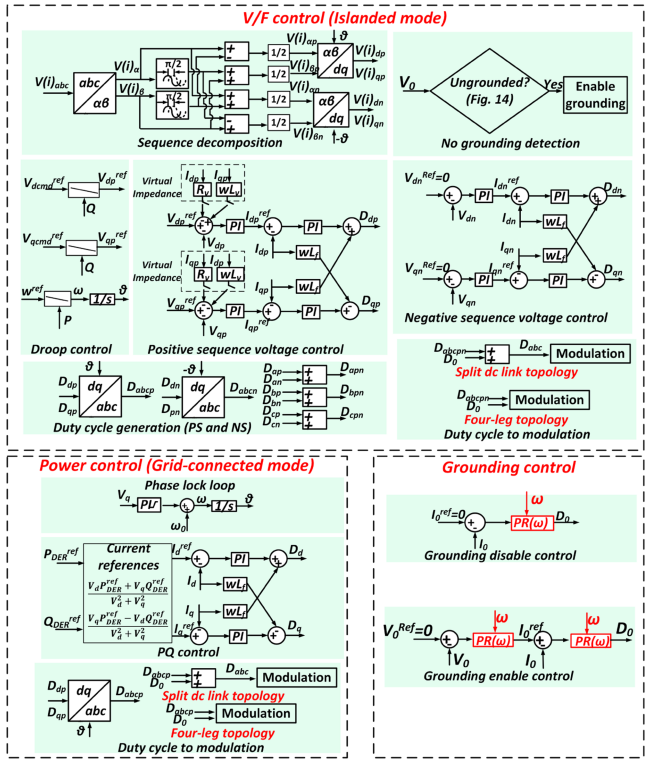

Fig. 11. Control algorithms.

C. Control Strategies of the DER Inverter for Grounding

The overall control logic of the DER inverter with grounding capability is summarized in Fig. 10. The DER inverter operates in the GFM mode in the islanded mode. In the grid-connected mode, the MG voltage and frequency are provided by the main grid, and the DER inverter is in the GFL mode to provide more flexibility for the power control. The DER inverter can enable and disable the grounding based on the MG needs through the grounding control transition. Detailed control algorithms are shown in Fig. 11. The proposed control algorithm can be used in both 50 and 60 Hz MGs. This article will use 60 Hz MGs for the discussion.

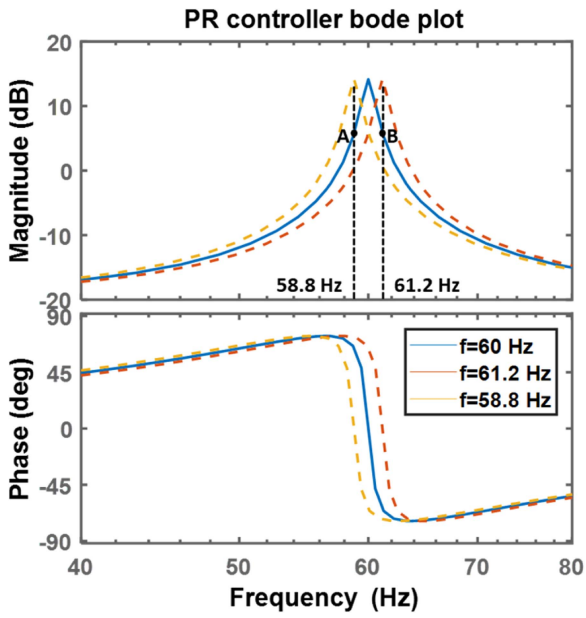

Fig. 12. PR controller bode plot under different resonant frequencies with $k_p = 0.1$, $k_i = 5$, and $\omega_{\text{cut}} = 0.5\times2\times\pi$.

1) Control in Grid-Connected Mode: In the grid-connected mode, the DER directly regulates its output active and reactive power based on MG requirements. The grid frequency and phase information are obtained from the phase lock loop (PLL). The DER inverter does not provide a grounding in the grid-connected mode to avoid the impacts on the main grid. The ZS current of the DER inverter is controlled to zero through a non-ideal proportional-resonant (PR) controller

$$PR\ (s) = K_P\ + \frac{2K_R\omega_{cut}s}{s^2 + 2\omega_{cut}s + \omega^2} \tag{11}$$

where ω equals the line frequency of the MG, which is supposed to be 60 Hz. However, in power grids, especially small grids like MGs, due to the frequency regulation, the frequency may not always be fixed at 60 Hz. According to IEEE Std. 1547-2018 [22], the continuous operation range of the frequency is 58.8–61.2 Hz. The PR controller has the highest gain at its resonant frequency. If the resonant frequency of the controller is fixed at 60 Hz, the controller cannot realize its highest gain when the fundamental frequency deviates from 60 Hz. As shown in Fig. 12, if the resonant frequency of the ZS is fixed at 60 Hz, when the line frequency deviates to 58.8 or 61.2 Hz, the gain of the controller will change to points *A* and *B*, which may impact the ZS regulation performance.

In order to solve this issue, an adjustable PR controller is applied. The grid frequency is detected by the PLL, and the detected frequency is applied to update the resonant frequency of the PR controller to improve the ZS regulation performance.

2) Control in Islanded Mode: In the islanded mode, the DER inverter operates in the GFM mode to form the MG voltage and frequency. PS and NS voltages are controlled separately in *dq* coordinates. The detailed sequence decomposition algorithm can be found in [23]. For the PS control, two perspectives

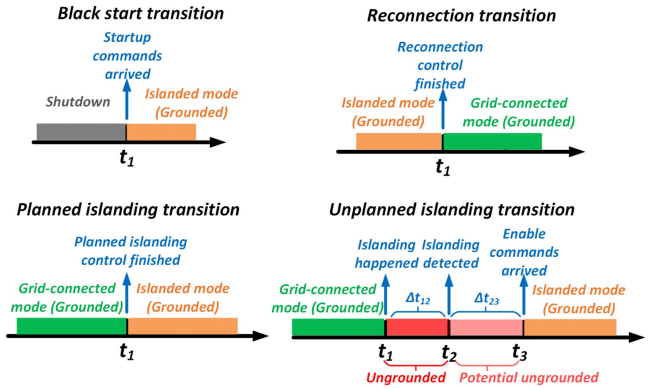

Fig. 13. Grounding transition timelines for the proposed scheme.

are considered. The first perspective is frequency regulation. Primary droop control is applied for the frequency regulation. The second perspective is power sharing. In MGs, the impedances and the X/R ratios of lines are small, resulting in inaccurate power sharing among multiple GFM inverters. To improve the power-sharing accuracy, virtual impedance control is applied, where the detailed analysis is covered in [24]. The NS voltage may cause damage to the three-phase loads such as motors, so the NS control target is to regulate the NS voltage to zero.

The grounding-enable control is applied in the islanded mode by regulating the ZS impedance to zero. One direct way is to regulate the ZS voltage to zero, where a dual loop control is applied. The nonideal PR controller in (11) with adjustable resonant frequency is also utilized in both inner and outer loops. In the islanded mode, the line frequency is regulated by the DER inverter through droop control. The controller resonant frequency is obtained from the frequency droop control.

3) Fault Condition: For the fault conditions, two cases need to be considered. First, assume the inverter can provide all the fault current. In this case, the inverter does not ride through. The ZS voltage caused by the fault current may result in TOV in the healthy phases. To meet the TOV requirement, the ZS impedance of the whole grounding scheme needs to be designed based on (6).

The second case is to assume that the inverter has a limited over-current capability. In this case, the inverter rides through the unbalanced fault, which may cause a voltage drop in the healthy phases. From the TOV perspective, the voltage drop in healthy phases will reduce the risk of exceeding the TOV limit. Therefore, this article will focus on the worst case that the inverter has sufficient current rating during faults. In this case, the control is the same as the steady state.

4) Transition Control: During mode transitions, the MG grounding is enabled/disabled by the inverter control that can respond within several semiconductor device switching cycles (<1 ms), therefore, the switching action delay can be neglected compared to the mechanical switches. The transition timelines for the proposed grounding approach are summarized in Fig. 13.

For the black start, planned islanding, and reconnection transitions, since the grounding switching is realized by the inverter

control, these transitions can be accelerated. Meanwhile, during the planned islanding and reconnection, the multineutral condition can be avoided to eliminate the potential impacts on the main distribution grid.

During the unplanned islanding transition, different islanding detection approaches can result in different ungrounded durations shown in Fig. 13. If the islanding detection is realized by the MG controller, the islanding event that happened at t_1 was detected at t_2, and transition commands are issued to DERs that arrived at t_3. The inverter then changed the control mode to the islanded mode. The grounding transition also ended with the control transition; the mechanical switching delay can be eliminated. Therefore, the transition time delay requirement is summarized as

$$\Delta t_{12} + \Delta t_{23} \leq T_{\text{TOV}}^{\max}. \tag{12}$$

DERs are also commonly applied for islanding detection, meaning that the communication delay Δt_{23} can be avoided. In this case, the transition duration is mainly determined by the islanding detection time. Once the islanding detection time is less than the maximum allowed TOV duration, the transition requirement can be met. In this article, passive detection is applied as an example of islanding detection [25]. The DER inverter monitors the grid voltage and frequency through PLL. Once the voltage and frequency cannot meet the steady-state requirement in [22] for a continuous period, the islanding will be detected, and the grounding transition will be executed. The islanding detection duration is applied to be two line cycles (32 ms) so that the TOV duration requirement can be met.

D. Operation of MG With Multiple Source Locations

In this type of MG, the proposed scheme can avoid additional transformers and switches to greatly reduce the cost. Also, the proposed approach can provide more flexibility for the MG grounding. In the grid-connected mode, all the inverters do not provide grounding. In the islanded mode, in a merged MG, since the grounding and neutral availability are determined by the inverter, the MG can either have multiple or single neutrals based on MG needs. If a single neutral is applied, the grounding transitions need to be considered. After the merging transition, only one inverter will enable the grounding. During the separation transition, the inverters that disabled the grounding in the merged MG will need to enable the grounding, which may result in the ungrounded condition and TOV. However, since multiple DER inverters all operate in the GFM mode, each sub-MG will not lose voltage source after separation, meaning that the passive detection may not be able to detect the separation accurately. Therefore, a grounding detection strategy is proposed, which is shown in Fig. 14. The no grounding condition is detected by the ZS voltage amplitude. When the ZS voltage is lower than 0.05 p.u., the MG can be viewed as grounded. When the ZS voltage is greater than 0.38 p.u., the MG may have extremely unbalanced conditions such as fault, which requests a fast response of the inverter to enable the grounding. Therefore, the minimum detection time should be smaller than the typical fault-clearing time ($t_{unG} < 0.2$ s). For a conservative design, in this article,

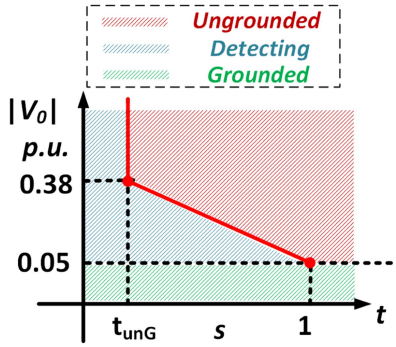

Fig. 14. Grounding detection strategy.

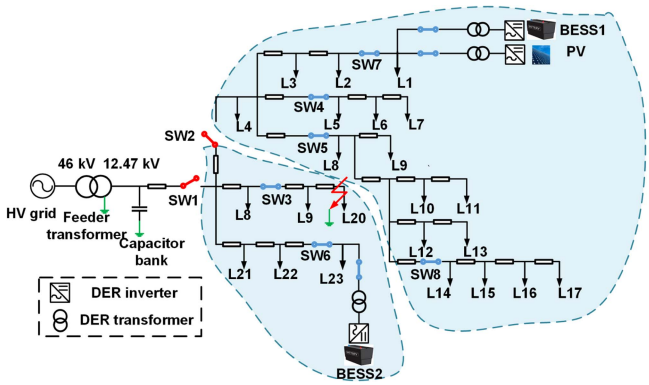

Fig. 15. Example MG topology from PNNL.

the minimum detection time is selected to be the same as the islanding detection time. When the ZS voltage is between 0.05 and 0.38 p.u., the detection time is inverse to the ZS voltage amplitude.

V. Simulation Verification

As shown in Fig. 15, the simulation is applied to the MG model from the Taxonomy Feeders developed by Pacific Northwest National Laboratory (PNNL) [26]. The MG parameters are shown in Table I. Two BESS inverters are GFM-controlled to regulate the MG voltage and frequency in the islanded mode. Sub-MG 1 is supported by BESS 1 and PV, and sub-MG 2 is formed by BESS 2. Two sub-MGs can be merged into one MG at switch SW 2. The grounding impedance is assumed to be 1 Ω. The BESS inverters are four-leg ones to work as groundings in the islanded mode.

A. Grounding Implementation

According to Fig. 9, the transformer impedance range can be calculated based on the steady-state voltage requirements. From the transformer voltage drop requirement, the calculated impedance range is $Z_T \leq 13.89\ \Omega$. According to the voltage unbalance requirement, the calculated impedance range is $Z_T \leq 43.58\ \Omega$. According to the design simulation, when the DER transformer impedance is 13.89 Ω, the TOV is less than its requirement. Therefore, the DER transformer impedance is

TABLE I
MG INFORMATION

Items	Information
MG voltage	12.47 kV
DER number	3 (2 BESSs, 1 PV)
BESS rating	600 kVA each
PV rating	2 MVA
BESSs transformer	480 V–12.47 kV, 600 kVA, Yg-Yg connection
PV transformer	480 V–12.47 kV, 2 MVA, Delta (MV) -Yg (LV) connection 5% impedance
Sub-MG 1	Source: BESS 1 +PV Load sections: L1– L17 Load ZS current: 4.95 A
Sub-MG 2	Source: BESS 2 Load sections: L18– L23 Load ZS current: 3.31 A

TABLE II
SUMMARY OF INVERTER-BASED GROUNDING SCHEME DESIGN

Items	Information
BESS1 transformer	Continuous rating: 35.39 A Thermal rating: 477.4 A Impedance: 13.89 Ω (X/*R* = 4)
BESS1 inverter	Current rating: 12.402 kA Voltage rating: 541 V ZS Current rating: 5.92 kA
BESS2 transformer	Continuous rating: 35.39 A Thermal rating: 477.7 A Impedance: 13.89 Ω (X/*R* = 4)
BESS2 inverter	Current rating: 12.409 kA Voltage rating: 541 V ZS Current rating: 5.87 kA

As a result, the thermal rating of the DER transformer and the DER inverter rating can also be selected. The DER transformer and inverter selections are summarized in Table II.

selected as 13.89 Ω. After the DER transformer impedance is selected, the maximum fault current rating can be determined. As a result, the thermal rating of the DER transformer and the DER inverter rating can also be selected. The DER transformer and inverter selections are summarized in Table II.

B. Grid-Connected Mode

In the grid-connected mode, all the DER inverters should not be applied as the MG grounding, therefore, the ZS currents for all the DER inverters are controlled to zero. The simulation results during the normal operation are shown in Fig. 16(a). The results show that in normal operation, all the ZS currents are provided by the main grid grounding. Two BESS do not provide ZS current.

The single-phase line-to-ground fault is also simulated in Fig. 16(b). The fault location is shown in Fig. 15. In the ground fault condition, the inverters are still able to regulate the ZS current to be close to zero. The ZS current provided by the inverters can be neglected compared to the ZS current provided by the grounding of the main grid. Therefore, the grounding

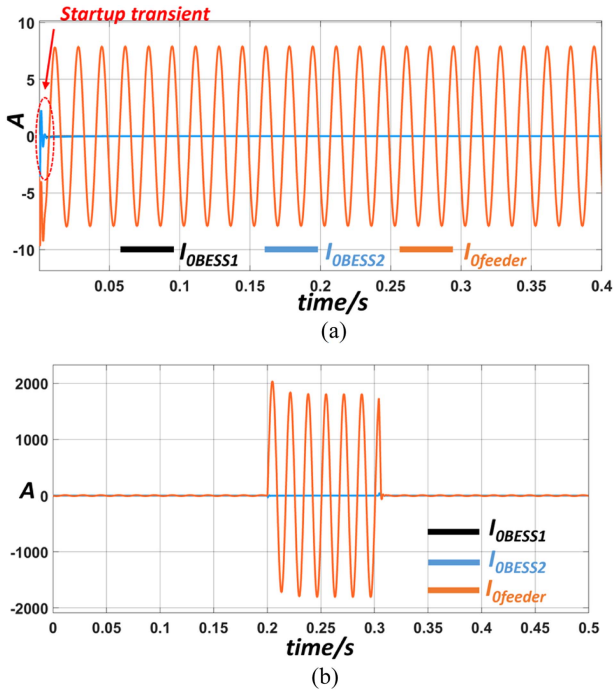

Fig. 16. Simulation results in grid-connected mode. (a) ZS current distribution in normal operation. (b) ZS current distribution in fault condition.

of the main grid still works as the only grounding in the fault condition.

C. Islanded Mode

1) Steady-State Case: In this case, two BESSs operate in a merged MG but only BESS1 works as the MG grounding. The simulation results are shown in Fig. 17. The output voltages of two BESSs are both balanced, which meets the requirement in (1). BESS1 provides PS, NS, and ZS current while BESS2 only provides PS and NS current, which demonstrates that the grounding capability is controllable in the islanded operation.

2) Fault Case: In this case, two BESSs still form a merged island, and only BESS1 provides the grounding. Single-phase line-to-ground fault is applied to phase *a*. The simulation results are shown in Fig. 18. A fault was applied at 0.2 s and was cleared at 0.3 s. The fault current was provided by two BESSs. The fault current in the islanded mode was smaller than the grid-connected operation because the BESS transformer impedance is higher than the grid-side impedance. During the fault condition, TOV occurred, and the TOV value was around 1.2 p.u., which meets the TOV requirement in (5). The ZS current was all supported by BESS1, meaning that BESS1 worked as a valid grounding while BESS2 was not the grounding. The inverter-based grounding is controllable in the fault condition.

D. Transitions

The transition process is shown in Fig. 19 and simulation results are shown in Fig. 20. In the two separate sub-MGs case, both BESSs worked as the grounding. The merging transition

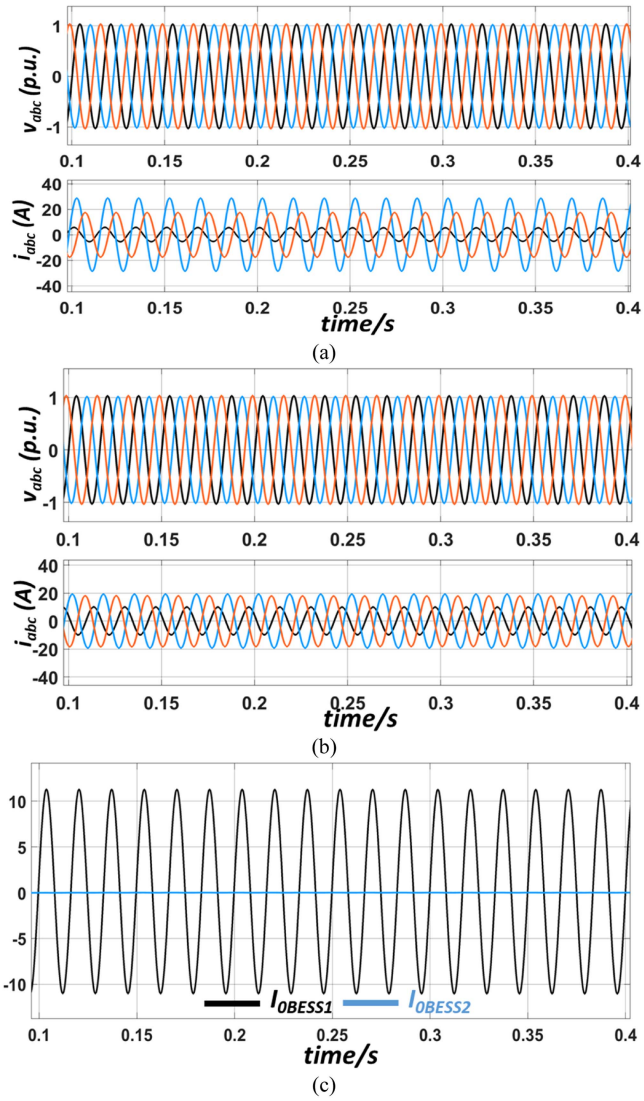

Fig. 17. Simulation results in islanded mode case 1). (a) BESS1 voltage and current. (b) BESS2 voltage and current. (c) ZS current distribution.

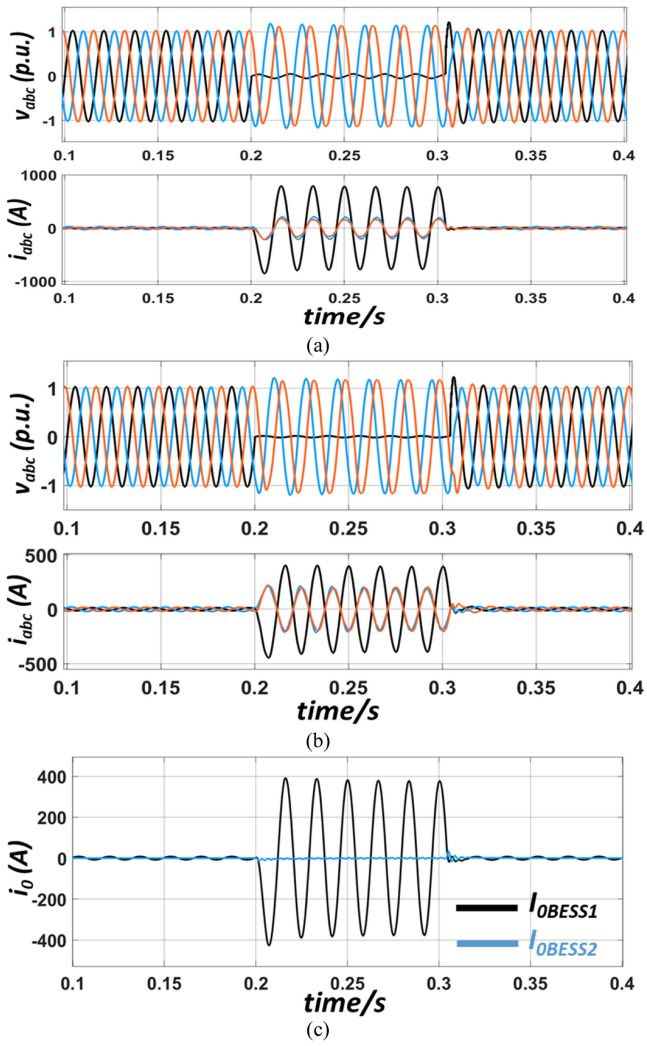

Fig. 18. Simulation results in islanded mode case 2). (a) BESS1 voltage and current. (b) BESS2 voltage and current. (c) ZS current distribution.

happened at t_1 when two sub-MGs merged into one, and the two BESSs gradually shared the ZS current equally. Grounding disabling transition happened at t_2. When the grounding function of BESS2 was disabled, BESS1 took over all the ZS current. During the transition process, the BESS voltage could be regulated to be balanced. The reconnection transition happened at t_3, two BESSs did not work as grounding and ZS current was controlled to be zero. The islanding transition happened at t_4, where an unplanned islanding event was simulated. The switch SW1 was opened at t_4 while the BESS inverters changed the operation mode at t_5. The MG lost the voltage source between t_4 and t_5. The MG voltage had a distinct drop, which triggered the islanding detection function to switch the mode.

The separation transition happened at t_6. An unplanned separation transition is simulated. Before t_6, only BESS1 worked as the grounding of the merged MG. Switch SW2 opened at t_6, and the BESS2 enabled the grounding capability at t_7. Between

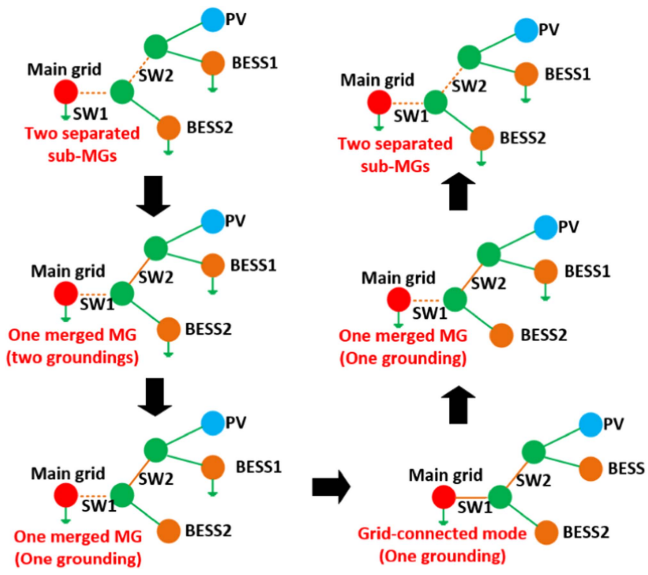

Fig. 19. Transition process.

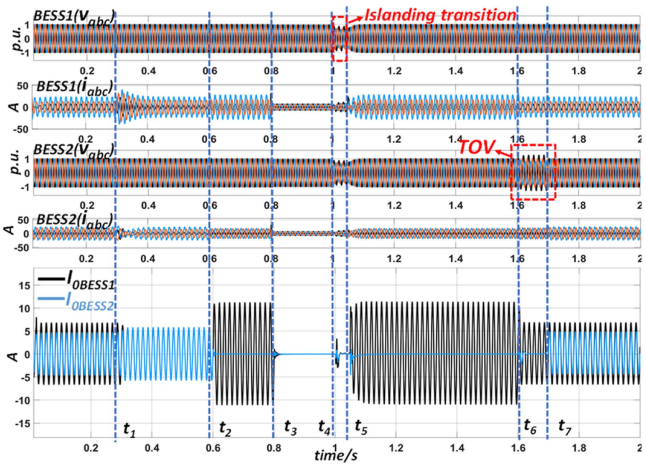

Fig. 20. Transition simulation results.

t_6 and t_7, there was no grounding in sub-MG 2. The voltage of BESS2 became unbalanced and TOV occurred. Therefore, the localized detection function in Fig. 14 was executed to enable the grounding function of BESS2 and provided sub-MG 2 with grounding at t_7.

E. Validation in 50 Hz MGs

The proposed grounding scheme is also validated in the 50 Hz MG scenario. The same MG topology in Fig. 15 is applied for simulation, where the operation frequency is changed to 50 Hz. The simulation results are summarized in Fig. 21, where grid-connected and islanded operations are simulated. The simulation includes steady-state and fault conditions. As shown in Fig. 21(a), in the grid-connected mode, the grounding is only provided by the main grid. In the islanded mode shown in Fig. 21(b) and (c), the grounding provided by the DER inverter can limit the voltage unbalance and TOV in the steady state and fault condition, respectively. It should be noted that the fault currents in the 50 Hz MG are higher than the 60 Hz MG. This is because the equivalent line impedance at 50 Hz is smaller than the line impedance in the 60 Hz MG.

F. Comparison With Existing Approaches

1) DER Transformer Approach: To compare with the DER transformer approach, the DER transformer connections are changed to Δ-Yg connections (Yg at MG side) so that DER transformers can serve as grounding. In the simulation, the numbers of the DER transformer-based grounding are changed to demonstrate the impacts of the DER transformer-based grounding scheme. Grid-side ZS current during single phase-to-ground fault conditions in the grid-connected mode are measured and summarized in Table III.

According to the measured ZS current magnitude, when all the DER transformers serve as the grounding of the MG, the fault ZS current at the grid side will reduce by 20.7% compared with the case that no DER transformer serves as the grounding in the grid-connected mode (the proposed grounding scheme). The grid-side ZS current change will impact the grid-side protection.

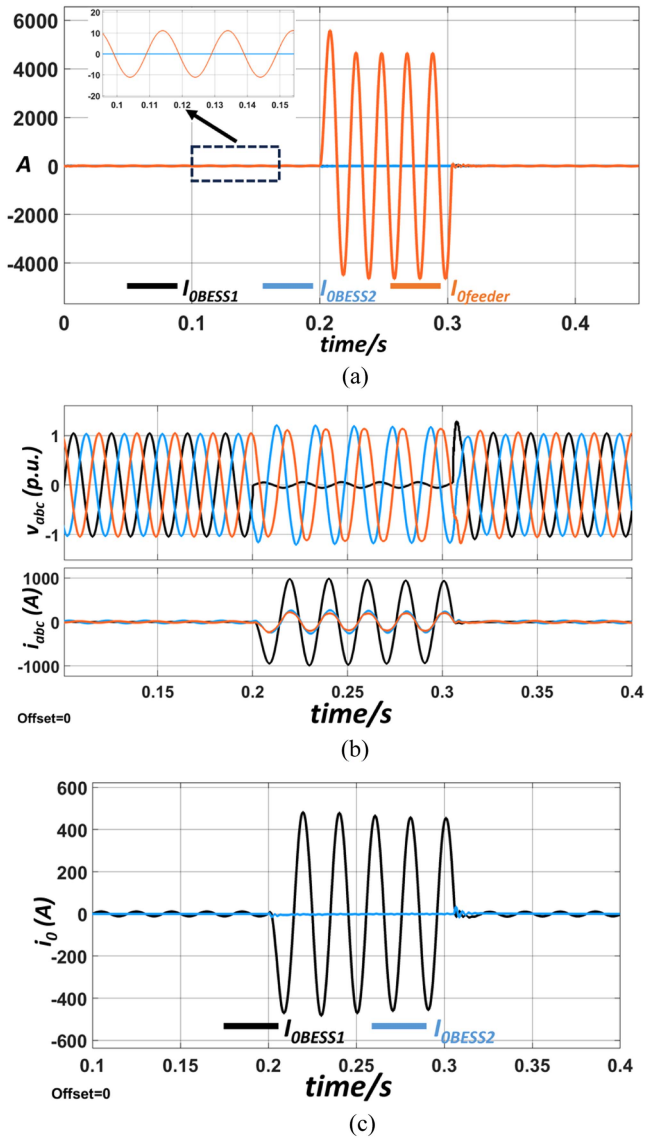

Fig. 21. Simulation results in 50 Hz MG. (a) ZS current distribution in grid-connected mode. (b) BESS1 voltage and current in islanded mode. (c) ZS current distribution in islanded mode.

TABLE III
ZS CURRENT MAGNITUDE UNDER DIFFERENT DER TRANSFORMER GROUNDING CONDITIONS

Grounding number	No DER grounding	One DER grounding	Two DER grounding	Three DER grounding
ZS current (A)	1750	1615	1498	1387

The proposed grounding scheme can avoid the impacts on the main grid.

2) Grounding Transformer Approach: Compared with the grounding transformer approach, the proposed grounding scheme can avoid specifically added grounding transformers. Moreover, the transition performance can also be improved. For the grounding transformer approach, the transition process in Fig. 19 is also simulated. Results are shown in Fig. 22. The

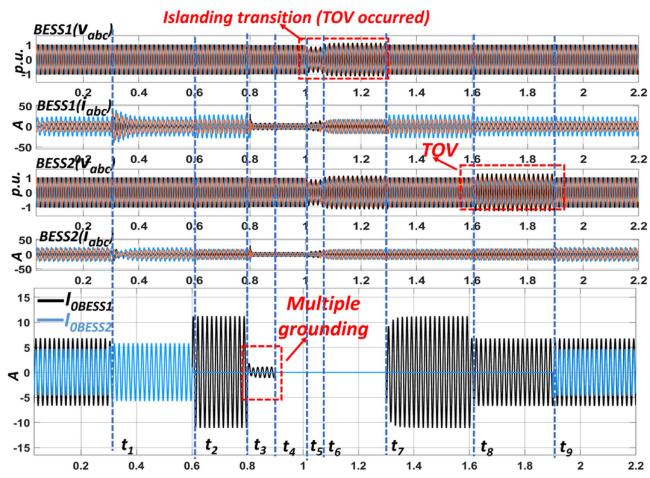

Fig. 22. Transition simulation results of the grounding transformer approach.

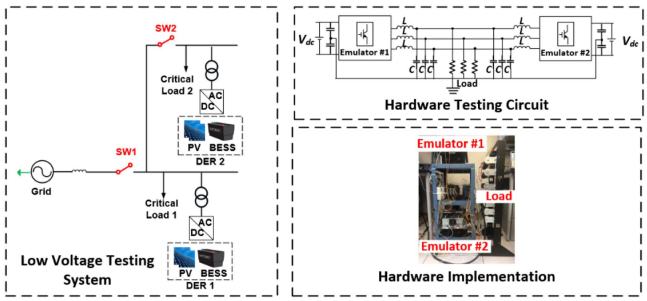

Fig. 23. Experimental setup of inverter-based MG grounding testing.

grounding transition follows the process in Fig. 7. During the reconnection transition, the MG reconnected to the grid at time t_3, and the grounding was disconnected at time t_4. During t_3 and t_4, there were multiple groundings in the grid, which may affect the protection if a ground fault occurs during this period. The unplanned islanding happened at time t_5 and was detected at t_6. However, due to the grounding transition delay (communications and mechanical actions), the grounding transition finished at t_7. During t_6 and t_7, the TOV occurred because of the ungrounded condition. The unplanned island separation transition happened at t_8 and finished at t_9. The grounding transition delay caused a longer TOV duration than the proposed approach. Overall, during the transition process, the grounding transition delays will cause multiple grounding and worse TOV conditions compared with the proposed approach.

VI. Experimental Verifications

Experimental testing is conducted for control algorithm validation. The testing is conducted on a converter-based hardware testbed (HTB), which is shown in Fig. 23. The converter in the experimental testing is a commercial converter from Vacon. The device in the converter is IGBT SEMiX202GB12E4s. The HTB is used to emulate an LV MG. The testing parameters and operating conditions are summarized in Table IV. Based on the testing parameters, the Bode plots of the ZS controller are shown in Fig. 24. The voltage and current levels of the testing are selected considering the equipment limitations. Two converter emulators are applied. Converter emulator #2 is the converter for proposed control testing whereas converter emulator #1 supports the testing. The experimental testing includes the steady-state conditions, transitions in a single MG, and transitions in the MG with multiple source locations. Before the actual experimental testing, simulation verification of the low voltage MG scenario is also conducted to serve as a benchmark of the experimental testing.

TABLE IV
Parameters of Testing Setup

Items	Parameters
Dc voltage rating	120 V
Ac voltage (peak)	54 V
Rated power	1146 W
Line frequency (f)	60 Hz
Filter values	L = 300 μH, C = 150 μF
Load conditions	R_a = 10 Ω, R_b = 10 Ω, R_c = 2.4 Ω
Emulator #1 (Supporting inverter)	Grid-connected mode: Grid Single MG case: Shut down Multiple sub-MGs case: GFM DER
Emulator #2 (Testing inverter)	DER emulator with grounding control

A. LV MG Simulation

In the LV MG simulation, two cases are considered. The first case is a transition from the steady-state grid-connected operation to the steady-state islanded operation, including an unplanned islanding transition. As shown in Fig. 25, before, the MG was in grid-connected operation. The ZS current is only provided by the main grid. After t_2, the MG is in islanded mode, and the grounding is provided by the DER inverter. The main grid supply was lost at t_1, and the islanding detection detected the disconnection of the grid at t_2. The DER mode transition and grounding enabling happened at t_2.

The second case is an islanding separation transition during the islanded mode. The simulation results are shown in Fig. 26. Before time t_1, the MG was formed by two DERs and only DER1 enabled the grounding. All the ZS currents are provided by DER1. At time t_1, the MG separated into two sub-MGs, and the sub-MG formed by DER2 no longer had any grounding resulting in its voltages becoming unbalanced. DER2 detected the no-grounding condition at time t_2 and enabled the grounding accordingly. After the grounding was provided, the voltage unbalance was limited to the acceptable range.

B. Steady-State Conditions

In the grid-connected mode, the grounding and neutral of the MG are provided by the main grid. Converter emulator #1 ran an open-loop voltage control to serve as the grid, and emulator #2 (DER) operated in the GFL mode to provide the grid with power. The testing results are shown in Fig. 27(a). The ZS voltage

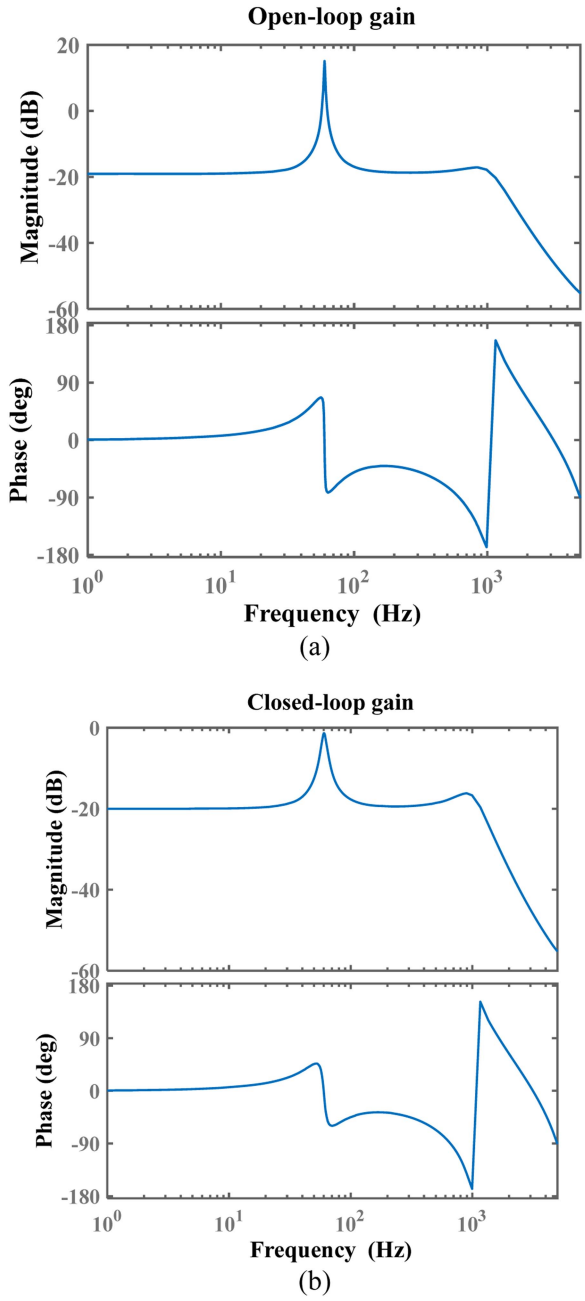

Fig. 24. Bode plots of the ZS controller. (a) Open-loop gain. (b) Closed-loop gains.

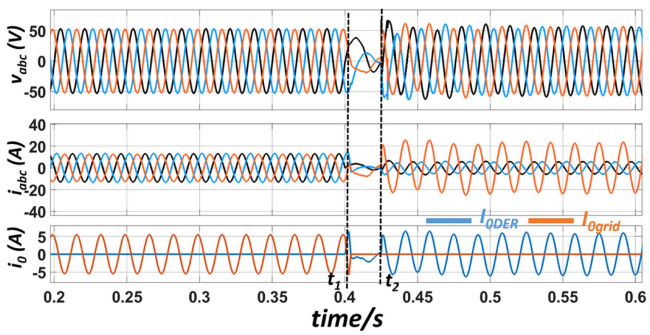

Fig. 25. Simulation results of case 1 in LV MG.

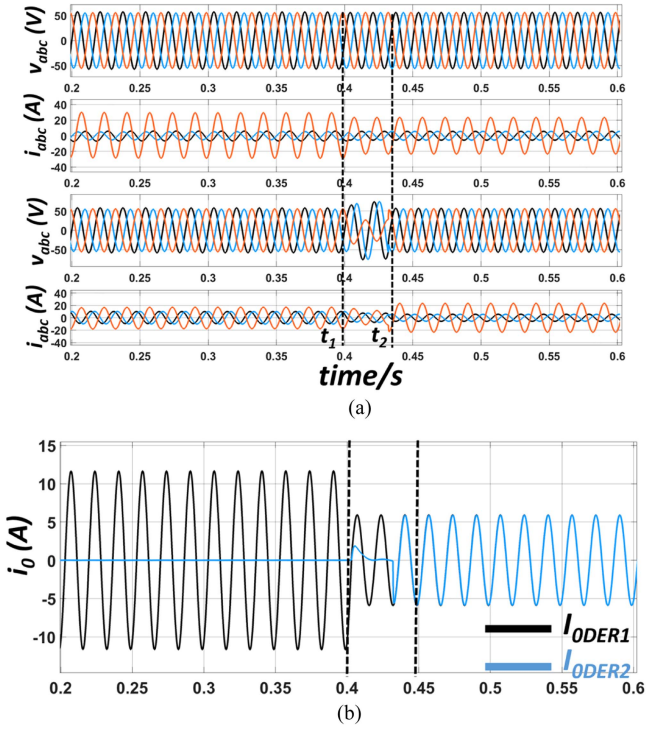

Fig. 26. Simulation results of case 2 in LV MG.

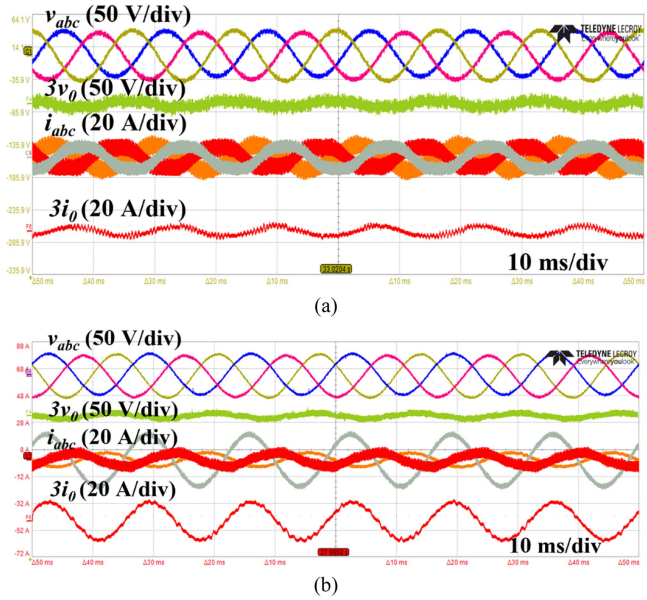

Fig. 27. Emulator #2 measurements in steady-state conditions. (a) Grid-connected mode. (b) Islanded mode.

and neutral current of the DER emulator were measured. The majority of the ZS current was provided by the grid emulator, and the ZS voltage met the requirement in (1). The ZS current of the DER emulator is not fully regulated to zero. This is because of the controller digitalization in DSP hardware (F28335) and the ADC resolution limitations. The gain of the PR controller is not infinite, resulting in a static error in the ZS current control. However, the ZS current of the DER emulator is much smaller

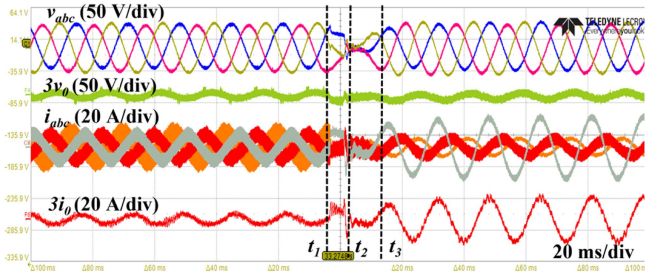

Fig. 28. Emulator #2 measurements in islanding transition in the single MG.

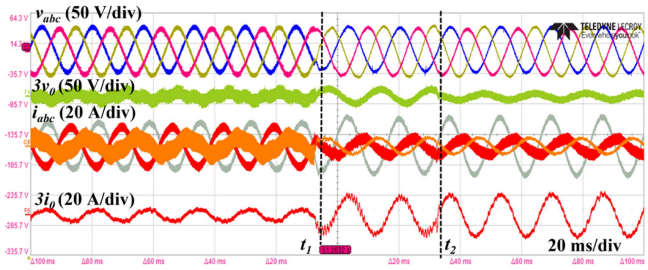

Fig. 29. Emulator #2 measurements in sub-MG separation transition.

than the grid emulator. The grounding is provided by the grid emulator. In the islanded mode, as shown in Fig. 27(b), the DER emulator served in the GFM mode, and the grounding control was enabled. Converter emulator #1 was shut down in this case. The DER emulator provided a ZS current path and the ZS voltage was limited to meet the requirement in (1).

C. Transition in MG With a Single Source Location

The unplanned islanding transition has an ungrounded condition. Therefore, the unplanned islanding transition is selected for the transition demonstration. During the transition, the grid emulator (emulator #1) was shut down manually to emulate a sudden outage of the grid. The testing results are shown in Fig. 28. The grid was lost at time t_1. Then the DER emulator detected the islanding condition at t_2 based on grid voltage and frequency deviation during t_1 and t_2. The DER emulator changed the operation mode to GFM mode and enabled the grounding control. The control transient ended at t_3, and the MG operated in the steady-state islanded mode. Therefore, the DER emulator can realize the grounding transition.

D. Transition in MG With Multiple Source Locations

In this case, two emulators both operate in the GFM mode to form a merged MG. The unplanned separation transition is tested for the sub-MG formed by emulator #2. Testing results are shown in Fig. 29. During this transition, before the transition happened, emulator #1 enabled the grounding control while emulator #2 disabled the grounding control. Emulator #1 was manually turned OFF at t_1 to emulate the separation. At this time, since emulator #2 was also in the GFM mode, the sub-MG formed by emulator #2 could still maintain the voltage and frequency while the grounding was lost, causing the ZS voltage and TOV. The no grounding detection of emulator #2 detected the ZS voltage and enabled the MG grounding at time t_2 to ensure the safe operation of the MG.

From the LV simulation and testing, the steady-state and transition capabilities of the proposed grounding scheme in the LV MG can be validated. Comparing the LV and MV simulation results, the proposed grounding scheme can both realize its grounding capability in the islanded mode, disable the grounding in the grid-connected mode, and realize fast grounding transitions as needed. Based on these comparisons, the proposed grounding scheme can also be applied to MV MGs.

VII. Conclusion

Existing transformer-based grounding schemes cannot meet all the transition requirements in MGs. The multineutral solution will affect the operation of the main grid while the single-neutral solution cannot meet the maximum allowed TOV duration requirement of the MG. In this article, a DER inverter-based MG grounding scheme is proposed. The detailed structure and equivalent ZS circuits for different MG operation modes are discussed. Control functions in different modes of the DER inverter are also illustrated. The proposed grounding scheme can avoid the impacts on the ZS current-based protection of the main grid. In addition, since the grounding availability is determined by the inverter control, the proposed approach can realize the fast grounding transition to greatly reduce the TOV duration during MG mode transitions. Therefore, the TOV duration requirement during transitions can be met. Simulation verification is conducted based on an actual MG topology for the system-level demonstration. Different MG operation modes, conditions, and transitions are simulated. The simulation results prove that the proposed MG grounding scheme works as the grounding in islanded mode while disabling the grounding in the grid-connected mode with smooth transitions. Experimental testing results are also conducted to verify the proposed control algorithms on actual hardware. The steady-state and transition controls are verified.

References

[1] *IEEE Recommended Practice for Grounding of Industrial and Commercial Power Systems*, IEEE Std. 142-2007 (Revision of IEEE Std. 142-1991), pp. 1–225, Nov. 2007.

[2] *IEEE Guide for the Application of Neutral Grounding in Electrical Utility Systems–Part IV: Distribution*, IEEE Std. C62.92.4-2014 (Revision of IEEE Std. C62.92.4-1991), pp. 1–44, Jan. 2015.

[3] IEEE Std. for Requirements, Terminology, and Test Procedures for Neutral Grounding Devices, IEEE Std. C57.32-2015 (Revision of IEEE Std. 32-1972), pp. 1–83, Apr. 2016.

[4] M. Pulcherio, M. S. Illindala, J. Choi, and R. K. Yedavalli, "Robust microgrid clustering in a distribution system with inverter-based DERs," *IEEE Trans. Ind. Appl.*, vol. 54, no. 5, pp. 5152–5162, Sep./Oct. 2018.

[5] S. Chanda and A. K. Srivastava, "Defining and enabling resiliency of electric distribution systems with multiple microgrids," *IEEE Trans. Smart Grid*, vol. 7, no. 6, pp. 2859–2868, Nov. 2016.

[6] R. H. Lasseter and P. Paigi, "Microgrid: A conceptual solution," in *Proc. IEEE 35th Annu. Power Electron. Specialists Conf.*, 2004, vol. 6, pp. 4285–4290.

[7] S. Zhen, Y. Ma, F. Wang, and L. M. Tolbert, "Operation of a flexible dynamic boundary microgrid with multiple islands," in *Proc. IEEE Appl. Power Electron. Conf. Expo.*, 2019, pp. 548–554.

[8] J. Mohammadi, F. B. Ajaei, and G. Stevens, "AC microgrid grounding strategies," in *Proc. IEEE/IAS 54th Ind. Commercial Power Syst. Tech. Conf.*, 2018, pp. 1–7.

[9] A. Vukojevic, "Lessons learned from microgrid implementation at electric utility," in *Proc. IEEE Power Energy Soc. Innov. Smart Grid Technol. Conf.*, 2018, pp. 1–5.

[10] L. Zhu et al., "A smart and flexible microgrid with a low-cost scalable open-source controller," *IEEE Access*, vol. 9, pp. 162214–162230, 2021.

[11] J. Chen, L. J. Diao, L. Wang, H. Du, and Z. Liu, "Distributed auxiliary inverter of urban rail train—The voltage and current control strategy under complicated load condition," *IEEE Trans. Power Electron.*, vol. 31, no. 2, pp. 1745–1756, Feb. 2016.

[12] Z. Lin, X. Ruan, L. Jia, W. Zhao, H. Liu, and P. Rao, "Optimized design of the neutral inductor and filter inductors in three-phase four-wire inverter with split DC-link capacitors," *IEEE Trans. Power Electron.*, vol. 34, no. 1, pp. 247–262, Jan. 2019.

[13] F. H. Md Rafi, M. J. Hossain, G. Town, and J. Lu, "Smart voltage-source inverters with a novel approach to enhance neutral-current compensation," *IEEE Trans. Ind. Electron.*, vol. 66, no. 5, pp. 3518–3529, May 2019.

[14] *IEEE Recommended Practice for Electric Power Distribution for Industrial Plants*, IEEE Std. 141-1993, pp. 1–768, Apr. 1994.

[15] A. K. Singh, G. K. Singh, and R. Mitra, "Some observations on definitions of voltage unbalance," in *Proc. 39th North Amer. Power Symp.*, 2007, pp. 473–479.

[16] *IEEE Guide for the Application of Neutral Grounding in Electrical Utility Systems–Part I: Introduction*, IEEE Std. C62.92.1-2016 (Revision of IEEE Std. C62.92.1-2000), pp. 1–38, Mar. 2017.

[17] *IEEE Guide for the Application of Metal-Oxide Surge Arresters for Alternating-Current Systems*, IEEE Std. C62.22-2009 (Revision of IEEE Std. C62.22-1997) - Redline, pp. 1–177, Jul. 2009.

[18] "Protection system reliability redundancy of protection system elements," North American Electric Reliability Corporation (NERC), Princeton, NJ, USA, Nov. 2008. [Online]. Available: https://www.nerc.com/comm/PC/System%20Protection%20and%20Control%20Subcommittee%20SPCS%20DL/Redundancy_Tech_Ref_1-14-09.pdf#search=Redundancy%5FTech%5FRef%5F1%2D14%2D09

[19] L. Zhang, H. Yang, K. Wang, Y. Yuan, Y. Tang, and W. K. Loh, "Design methodology for three-phase four-wire T-type inverter with neutral inductor," *CPSS Trans. Power Electron. Appl.*, vol. 6, no. 1, pp. 93–105, Mar. 2021.

[20] C. Tan, Q. Chen, L. Zhang, and K. Zhou, "Frequency-adaptive repetitive control for three-phase four-leg V2G inverters," *IEEE Trans. Transp. Electrific.*, vol. 7, no. 4, pp. 2095–2103, Dec. 2021.

[21] R. Ghosh and G. Narayanan, "Control of three-phase, four-wire PWM rectifier," *IEEE Trans. Power Electron.*, vol. 23, no. 1, pp. 96–106, Jan. 2008.

[22] *IEEE Std. for Interconnection and Interoperability of Distributed Energy Resources with Associated Electric Power Systems Interfaces*, IEEE Std. 1547-2018 (Revision of IEEE Std. 1547-2003), pp. 1–138, Apr. 2018.

[23] Y. Liang, "A new time domain positive and negative sequence component decomposition algorithm," in *Proc. IEEE Power Eng. Soc. Gen. Meeting*, 2003, vol. 3, pp. 1638–1643.

[24] H. Zhang, S. Kim, Q. Sun, and J. Zhou, "Distributed adaptive virtual impedance control for accurate reactive power sharing based on consensus control in microgrids," *IEEE Trans. Smart Grid*, vol. 8, no. 4, pp. 1749–1761, Jul. 2017.

[25] D. Menon and A. Antony, "Islanding detection technique of distribution generation system," in *Proc. Int. Conf. Circuit, Power Comput. Technol.*, 2016, pp. 1–5.

[26] K. P. Schneider et al., "Modern grid initiative distribution taxonomy final report," Pacific Northwest Nat. Lab., Richland, WA, USA, Nov. 2008.